IEEE Photonics Journal
An IEEE Photonics Society Publication

Open Access

Flexible Amorphous GeSn MSM Photodetectors

Volume 10, Number 2, April 2018

Firat Yasar
Wenjuan Fan
Zhenqiang Ma

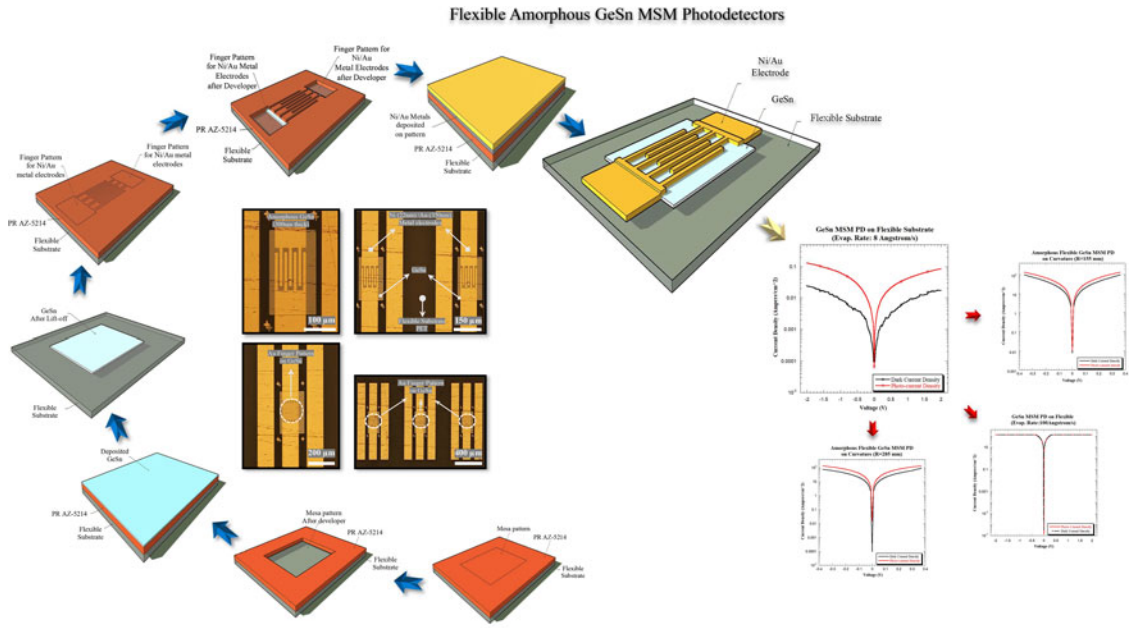

Graphical Abstract: Fabrication process illustrations, optical microscope images with dimensions, and current density graphs of flexible amorphous GeSn MSM photodetector.

DOI: 10.1109/JPHOT.2018.2804360
1943-0655

IEEE photonics SOCIETY

IEEE

Flexible Amorphous GeSn MSM Photodetectors

Firat Yasar,[1] **Wenjuan Fan**,[2] **and Zhenqiang Ma** [1,2]

[1]Materials Science Program University of Wisconsin-Madison, Madison, WI 53706 USA
[2]Department of Electrical and Computer Engineering, University of Wisconsin-Madison, Madison, WI 53706 USA

DOI:10.1109/JPHOT.2018.2804360

Manuscript received November 23, 2017; revised February 2, 2018; accepted February 6, 2018. Date of publication February 14, 2018; date of current version March 9, 2018. Corresponding author: Firat Yasar (e-mail: fyasar@wisc.edu).

Abstract: We demonstrate amorphous $Ge_{0.92}Sn_{0.08}$ surface illuminated metal–semiconductor–metal (MSM) photodetectors on flexible substrates for visible wavelength. Photodetection at 633 nm is achieved with an *I–V* response up to 10^{-4} A for a 2 V bias voltage. Different evaporation rate effects on the amorphous GeSn MSM photodetector are examined. Bending/strain effects on device performance were studied by evaluating the current density versus voltage characteristics. Amorphous GeSn thin film deposition on polyethylene terephthalate flexible substrate and Ni/Au–GeSn–Ni/Au MSM photodetector finger pattern deposition were performed via thermal evaporation. Photocurrent and dark current densities of amorphous GeSn MSM photodetectors were obtained at 1.36 A/cm^2 and 0.24 A/cm^2, respectively, where the photocurrent to dark current contrast ratio was found to be equal to 5.6. We also examined the evaporation rate, strain, and bending effect.

Index Terms: Flexible, amorphous, metal-semiconductor-metal (MSM), photodetectors, I–V curves, strain.

1. Introduction

For electronics and photonics integrated circuits, Silicon (Si) and Germanium (Ge) are widely-used materials, although these two group IV elements have indirect band gaps preventing them from being employed to realize light emitting components. In recent years, GeSiSn has emerged as a promising optoelectronic material. In principle, growing GeSn that is tensile-strained or lattice matched on Si substrate can realize a direct energetic transition in this kind of heterostructure system. Compressively strained GeSn on Ge exhibits intriguing optical absorption features to realize short wave infrared photodetectors while missing a direct band gap [1]. New progress in growth has been stated showing the achievement of a fully strained $Ge_{0.92}Sn_{0.08}$ layer on Ge, although the lattice mismatch between Ge and Sn is considerably large [2], [3]. The emission and absorption properties of these lattice-matched hetero-structures can be evaluated by this technological development. Demonstration of the use of a GeSn/Ge heterostructure-based photodetector in the short-wave infrared (SWIR) is very attractive for several applications including the field of spectroscopic sensing on gas, liquid, and solid absorption characteristics in SWIR [4]. Due to their compatibility with large-scale planar integrated circuit (IC) technology, MSM photodetectors are very appealing for various optoelectronic applications including upcoming high-speed chip-to-chip connection and high-speed sampling [1].

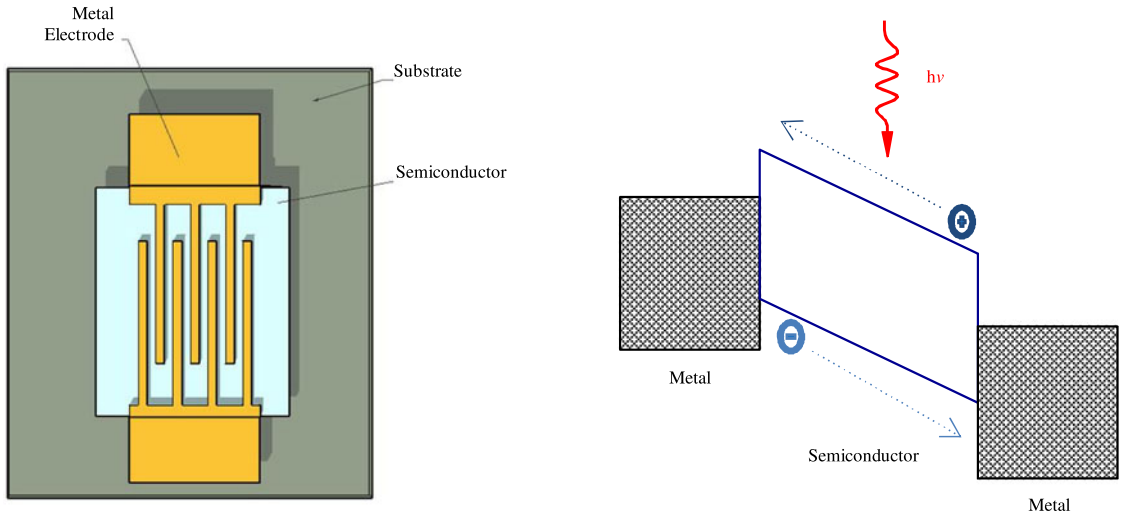

Fig. 1. Schematic view of a MSM photodetector and the band structure.

An MSM photodetector is a basic photonic device consisting of back-to-back Schottky diodes, as well as embodying interdigitated metal fingers on a semiconductor layer. MSM photodetectors are naturally planar devices that do not require complicated photolithography methods of fabrication. A schematic view of a MSM photodetector is shown in Fig. 1. A basic MSM photodetector employs a layer of semiconductor material sensitive to the desired wavelength. An energy band diagram is also shown in Fig. 1 for an MSM photodetector [5].

'Flexible integrated photonics' broadly implies photonic devices fabricated on flexible polymer substrates that can be mechanically deformed. This deformation might happen in various ways including bending, folding, rolling, twisting, stretching or compression without cooperation of the optical features of photonic devices [6], [7]. The emergence of applications such as flexible imaging/display arrays [8], [9], short-reach optical links [10], [11], wearable photonic textiles [12], [13], solar cells [14], [15], broadband tunable photonic devices [16], [17], strain gauges [18], [19], and optical systems conformally integrated on curved surfaces [20], [21] or biological tissues [22], [23]. In addition to their optical design concerns, the necessity of mechanical flexibility also leads to exclusive restrictions on material processing and mechanical engineering of flexible photonic devices. Because of their essential mechanical flexibility, polymers have been a favored material for flexible photonic devices for a long time. Polymers are also used for wave guiding [24], [25], filtering [26], light emission [27], [28], and optical modulation [29], in addition to serving as a flexible substrate material.

In this article, we present a flexible photonic device, which is an amorphous $Ge_{0.92}Sn_{0.08}$ MSM photodetector on polyethylene terephthalate (PET) flexible substrate. The paper is organized as follows; we first clearly explain device fabrication, which includes advanced lithograph and deposition techniques, etc. Then we explain the measurement of the device performance and discuss the results. The paper concludes with an evaluation of the device and results.

2. Device Fabrication

Both GeSn mesa fabrication and Ni/Au metal electrode fabrication follow two repeated sets of steps. These steps include sample cleaning, lithography and patterning, thin film deposition, and lift-off. Polyethylene terephthalate (PET) flexible substrates are used for amorphous GeSn MSM PD fabrication. As a beginning step in the first half of device fabrications, flexible (PET) substrates were exposed to ultrasonic cleaning for 7 minutes using acetone and subsequently isopropanol, followed by a rinse with DI water for 1 min. Cleaned, lithography-ready substrates were exposed to

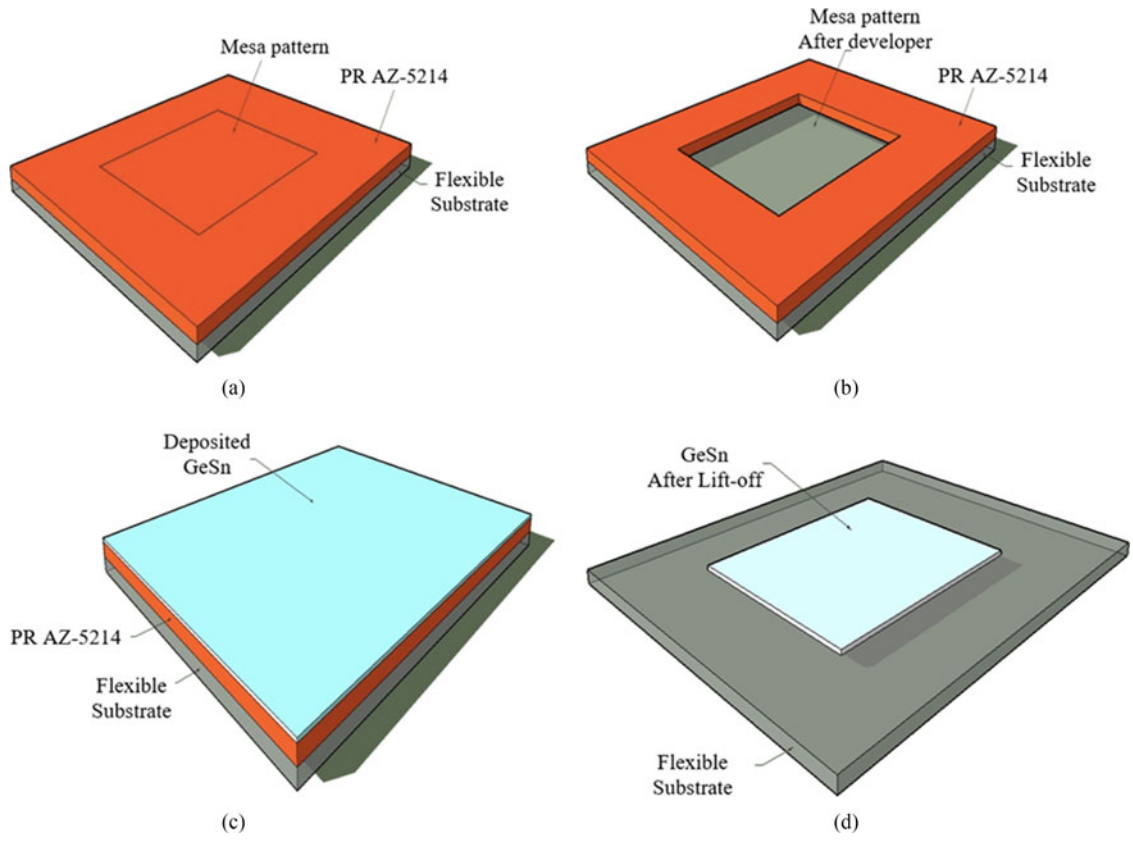

Fig. 2. A schematic diagram for the first half of flexible GeSn MSM photodetector fabrication. (a) Photo-resistor coated and mesa patterned flexible substrate. (b) Removed PR from patterned area by developer process for GeSn mesa deposition. (c) Deposited amorphous GeSn by thermal evaporation onto patterned PR on flexible substrate. (d) Obtained amorphous GeSn mesa on flexible substrate after lift-off process.

HMDS chemical gas solution to increase substrate surface stuffiness of photoresist (PR). Then AZ 5214 PR was coated using a spinner. To obtain a specific thickness, PR AZ 5214 was coated for 30 s at 4000 rounds per minute (rpm) angular velocity. PR AZ 5214 coated substrates were then baked for 3 min at 90 °C degrees. Substrates are exposed to ultra-violet (UV) light by an MJB-3 aligner for 2.5 s under a mask with basic rectangular patterns for GeSn mesa. Following UV light exposure, the substrates were baked for 90 s at 115 °C degrees. The samples were then directly, without a mask, exposed to UV light for 25 s [see Fig. 2(a)]. To obtain a patterned area without PR for GeSn deposition, MIF-917 liquid chemical solution, a developer, was applied for 30 s. This was immediately followed by a DI water rinse and applied to restrict the PR removal process with the desired pattern area [see Fig. 2(b)]. This PR coating process is called negative PR coating. In the first deposition step, bulk $Ge_{0.92}Sn_{0.08}$ material was deposited on the substrate by a thermal evaporator. A 300 nm thick GeSn thin film was deposited on mesa-patterned substrates by 8 Å/s, which is relatively faster than general thin film deposition. This fast evaporation approach arises from avoiding Sn segregation due to the large melting temperature differences between Ge and Sn, temperatures of 938.2 °C and 231.9 °C, respectively.

Similar to all other methods of thermal evaporation of thin films, amorphous crystalline $Ge_{0.92}Sn_{0.08}$ thin film was deposited at the end of this step [see Fig. 2(c)]. The entire surface of substrates was deposited with GeSn thin film; however, only the mesa region was needed. Thus, a simple hot acetone (75 °C) application was applied for several minutes to remove the PR thin film from the substrate, a procedure known as lift-off. As shown in the figure, only the 300 nm thick

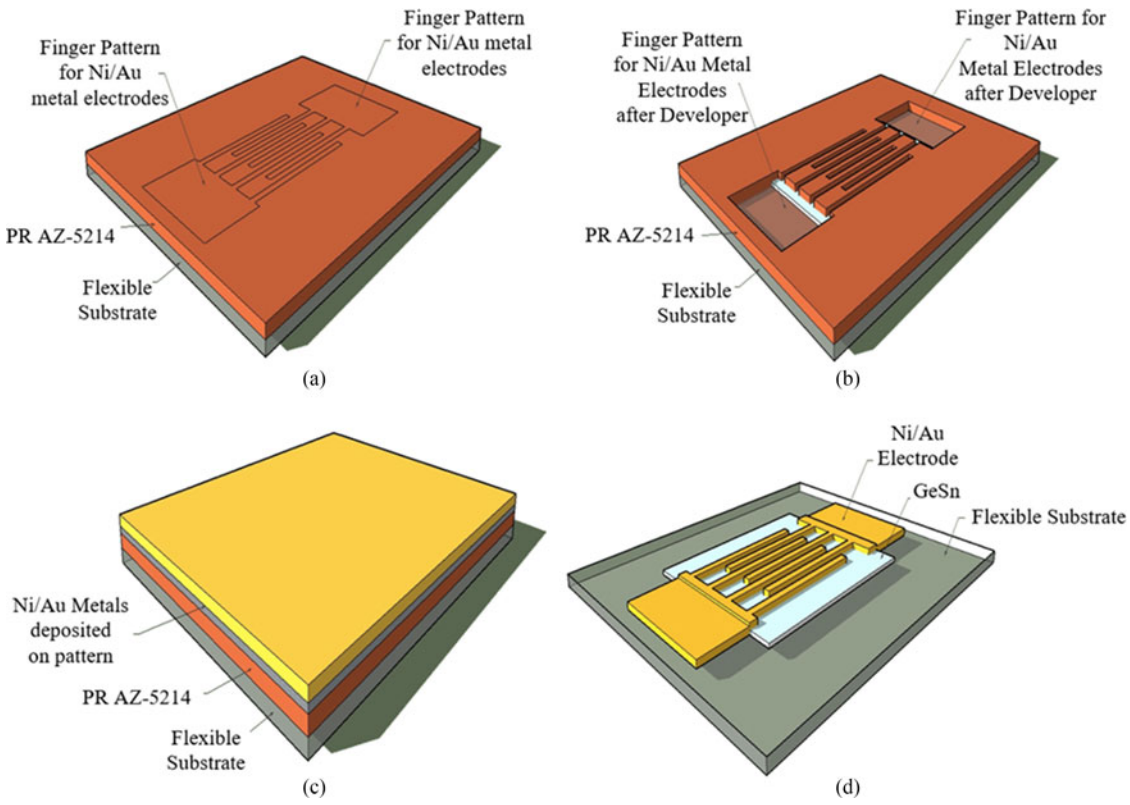

Fig. 3. A schematic diagram for the second half of flexible GeSn MSM photodetector fabrication. (a) Photo-resistor coated and finger patterned flexible substrate with amorphous GeSn thin film mesa. (b) Removed PR from patterned area by developer process for Ni/Au metal electrodes deposition. (c) Deposited Ni/Au finger shaped metal electrodes by thermal evaporation onto patterned PR on flexible substrate with amorphous GeSn thin film mesa. (d) Obtained amorphous Ni/Au finger shaped metal electrodes on flexible substrate with GeSn thin film mesa after second lift-off process.

GeSn (mesa) thin film remains on the substrates in the patterned region, at the end of the lift-off process [see Fig. 2(d)]. This process marks the end of the first half of device fabrication.

The remainder of device fabrication will be a repetition of the previous steps. It differs in the pattern for metal electrodes for canalizing the electrical current through mesa within the device. This pattern is called a finger pattern because of its shape which will help the aim mentioned above. The substrates were cleaned with Piranha solution to avoid possible damage to the GeSn thin film, followed by lithography. Finger pattern, which is located on the mask for metal electrodes, was used and carefully aligned with MJB-3 aligner [see Fig. 3(a)]. The sample was subjected to a second deposition of metal electrodes after MIF-917 developer application [see Fig. 3(b)].

This metal electrode deposition consists of two subsequent depositions of 25 nm thick Ni, then 350 nm thick Au. The total metal thickness should be larger than the mesa thickness to obtain continuity of conduction through metal electrodes. Deposition of the second half of fabrication is done via CHA-600 e-beam evaporator, which is comparatively slower than the mesa deposition by roundly 0.7 Angstrom/second [see Fig. 3(c)]. The second lift-off of metal fingers is the last step of device fabrication. The device is ready for performance measurements [see Fig. 3(d)].

In this article, we elaborate the current density (J) versus voltage characteristics of fabricated amorphous GeSn MSM photodetectors with Ni/Au electrodes on flexible substrates, which was measured in the dark environment (dark current) and under illumination (photocurrent). Illumination of a He/Ne laser with power of $\sim$10 mW at the incident wavelength of 633 nm is used for photocurrent measurements. Fig. 4 shows micro-graphs of fabricated device in different scales. GeSn mesa surface area of 3.0×10^4 μm^2 is used for current density calculations.

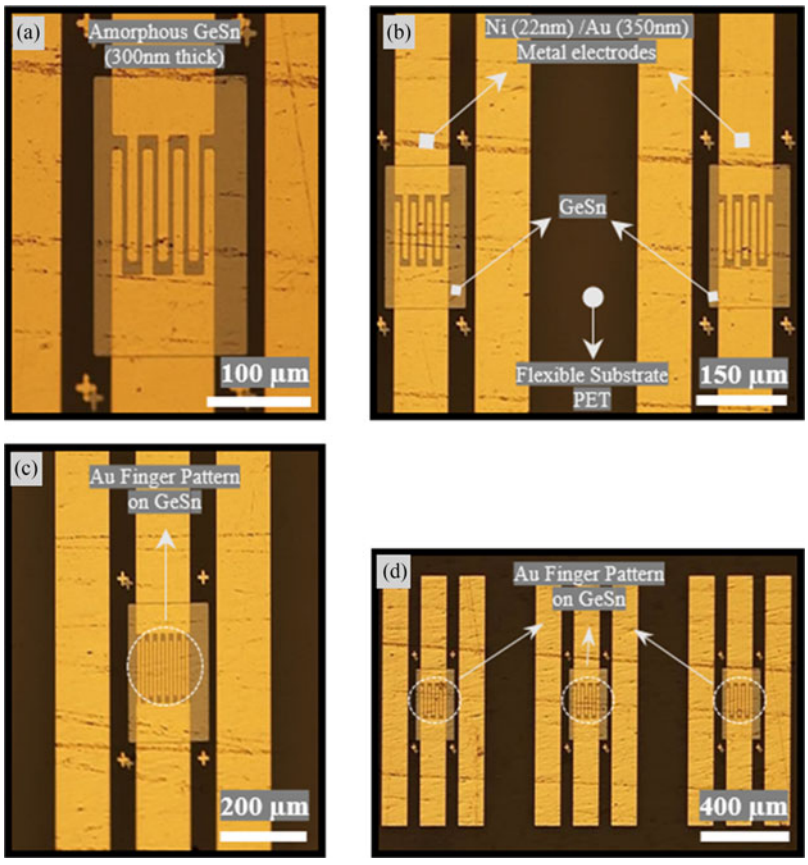

Fig. 4. (a), (b), (c) and (d) top view of flexible amorphous GeSn photodetector device in different scales.

3. Results and Discussion

Device measurements are done within two different categories. In the first category, the photo current response of amorphous GeSn MSM photodetectors on flexible substrates were measured. Three different GeSn mesas were deposited at evaporation rates of 8 Å/s, 100 Å/s, and 150 Å/s and the results were compared to each other based on these evaporation rates. Fig. 5 shows the photocurrent and dark current densities of an amorphous GeSn MSM photodetector on flexible substrate with GeSn mesa with an evaporation rate of 8 Å/s at 2 V applied bias.

For this device, a photocurrent and a dark current of 4.1×10^{-4} A and 7.3×10^{-5} A were measured, respectively. Current density values were calculated as 1.36 A/cm^2 and 0.24 A/cm^2 using a GeSn mesa surface of 3.0×10^4 μm^2. In other words, photocurrent to dark current ratio of 5.6 was measured. This ratio remained constant for current density calculations since both were subjected to the same surface area. In order to enhance the crystallographic features of amorphous GeSn mesa thin film and decrease Sn segregation adverse effects on MSM photodetector, GeSn mesa deposition is made at relatively faster evaporation rates of 100 Å/s and 150 Å/s. However, Sn segregation occurs even at faster evaporation rates given above due to a massive ($\sim$706 °C) temperature difference in melting points of Sn and Ge. Therefore, there is no photocurrent observed, and GeSn mesa semiconductor thin films exhibited no photo response at 100 Å/s and 150 Å/s evaporation rates, as can be seen from Fig. 6.

The strain effects on amorphous GeSn MSM photodetectors on flexible substrates were observed; in other words, we examined the current density versus voltage characteristics of this flexible photonic device by bending it. While the results of the relaxed amorphous GeSn MSM photodetector

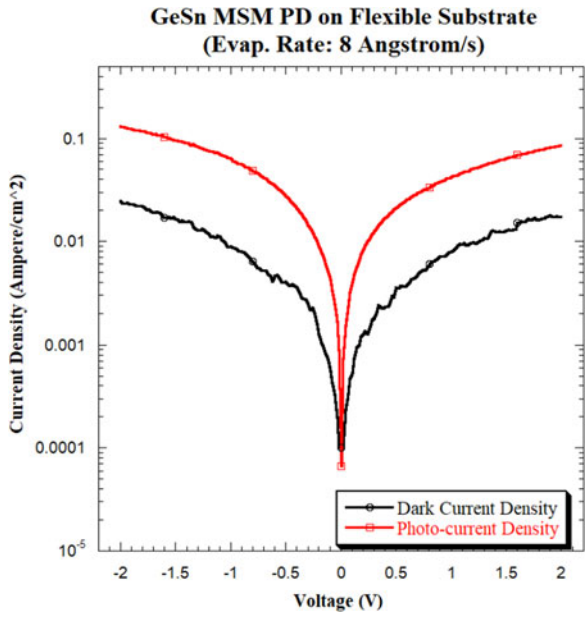

Fig. 5. Current density versus voltage characteristic of the fabricated GeSn MSM photodetector with Ni/Au electrodes on PET with deposited GeSn mesa at evaporation rate of approximately 8 Å/s.

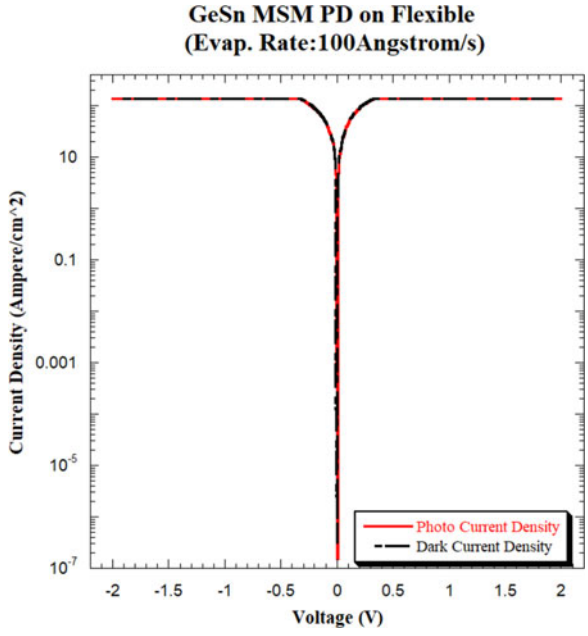

Fig. 6. Current density versus voltage characteristic of the fabricated GeSn MSM photodetector with Ni/Au electrodes on PET with deposited GeSn mesa at evaporation rate of approximately 100 Å/s.

on flat or non-bent flexible substrate can already be seen from Fig. 6, the results for bent flexible photodetectors, which are fixed at a spherical substrate holder to measure the bending effect, are shown in Figs. 7 and 8. With the bending effect of both at 285 mm and 155 mm diameter curvatures, flexible devices lose the photo current response at the edges of the applied voltage bias, but just near the zero-voltage value including both negative and positive regions. While showing much less photo response on the 285 mm diameter curvature than on the relaxed device, it almost shows no

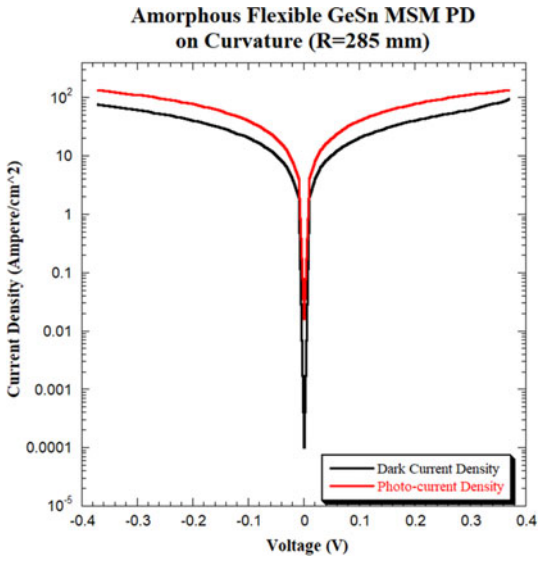

Fig. 7. Current density versus voltage characteristics of the fabricated GeSn MSM photodetector with Ni/Au electrodes on PET with deposited GeSn mesa at spherical substrate holder with 285 mm diameter.

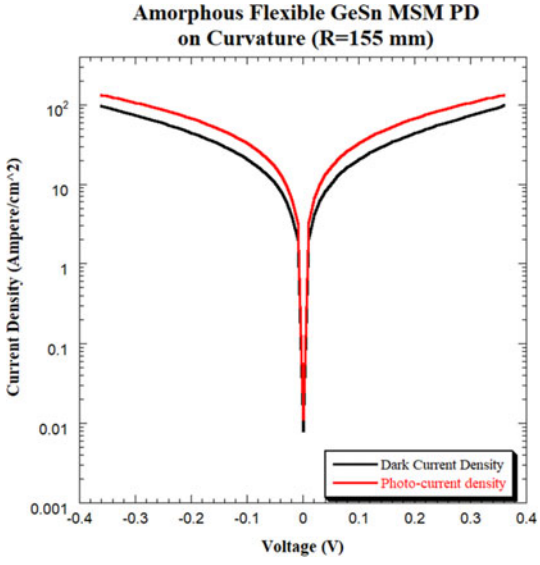

Fig. 8. Current density versus voltage characteristics of the fabricated GeSn MSM photodetector with Ni/Au electrodes on PET with deposited GeSn mesa at spherical substrate holder with 155 mm diameter.

photo-response with the increased bending effect on the 155 mm diameter curvature. Bending the amorphous GeSn MSM photodetector on flexible PET substrate has an obvious adverse effect on device performance and photo response. The results of bending effects on the flexible photodetector prove the formation of defects through the GeSn structure which results in a loss of photo-response. Generation of defects and irreversible deformation in the amorphous GeSn thin film structure under tensile strain is an indication of the inadequate mechanical durability causing low photo-current response.

4. Conclusion

In conclusion, we demonstrate an amorphous GeSn MSM photodetector with Ni/Au electrodes on flexible PET substrate. We examined different evaporation rate effects on the amorphous GeSn MSM photodetector. We also elaborate on the bending or strain effects on device performance by evaluating the I–V characteristics as well as current density versus applied voltage data. Amorphous GeSn thin films were deposited on PET flexible substrate by thermal evaporation. The Ni/Au-GeSn-Ni/Au MSM photodetector was then fabricated. It is found that the photocurrent and dark current of amorphous GeSn MSM photodetector is 4.1×10^{-4} A and 7.3×10^{-5} A, respectively, and the photocurrent to dark current contrast ratio was found to be equal to 5.6. The same ratio of 5.6 was also obtained after current density calculations were performed for both photo-current and dark current. The highest photocurrent-dark current ratio has been observed on the flat device with the lowest evaporation rate. Furthermore, it has been realized that the bending impact on photodetector and the higher evaporation rates of thin film deposition decreases the photocurrent-dark current density ratio.

In all, these results show that the fabrication of amorphous GeSn MSM photodetectors on flexible substrates operating at room temperature is possible by thermal evaporation. An amorphous GeSn flexible photodetector with metal-semiconductor-metal structure has been demonstrated for the first time. The amorphous structure provides an abundant choice of fabrication techniques including fabrication at relatively low temperatures. Moreover, it brings the advantages of simple and time efficient fabrication to very low cost, when compared with the fabrication of single crystalline thin films.

The author also would like to acknowledge the assistance offered and experiences shared by Prof. Dr. Zongfu Yu, Munho Kim, Jaeseong Lee, Minkyu Cho, Namki Cho.

References

[1] A. Gassenq *et al.*, "GeSn/Ge heterostructure short-wave infrared photodetectors on silicon," *Opt. Exp.*, vol. 20, pp. 27297–27303, 2012.
[2] F. Gencarelli *et al.*, "Low temperature Ge and GeSn chemical vapor deposition using Ge2H6," *Thin Solid Films*, vol. 520, no. 8, pp. 3211–3215, 2012.
[3] J. G. Crowder, S. D. Smith, A. Vass, and J. Keddie, "Infrared methods for gas detection," in *Mid-Infrared Semiconductor Optoelectronics*. New York, NY, USA: Springer, 2006.
[4] S. Y. Chen and M. Y. Liu, "Nanoscale tera-tertz metal–semiconductor–metal photodetectors," *IEEE J. Quantum Electron.*, vol. 28, no. 10, pp. 2358–2368, Oct. 1992.
[5] P. R. Berger, "MSM photodiodes," *IEEE Potentials*, vol. 15, no. 2, pp. 25–29, Apr./May 1996.
[6] J. Hu, L. Li, H. Lin, P. Zhang, W. Zhou, and Z. Ma, "Flexible integrated photonics: Where materials, mechanics and optics meet [Invited]," *Opt. Mater. Exp.*, vol. 3, pp. 1313–1331, 2013.
[7] W. Zhou *et al.*, "Flexible photonic-crystal Fano filters based on transferred semiconductor nanomembranes," *J. Phys. D*, vol. 42, no. 23, 2009, Art. no. 234007.
[8] H. C. Ko *et al.*, "A hemispherical electronic eye camera based on compressible silicon optoelectronics," *Nature*, vol. 454, no. 7205, pp. 748–753, 2008.
[9] L. Zhou, A. Wanga, S. Wu, J. Sun, S. Park, and T. Jackson, "All-organic active matrix flexible display," *Appl. Phys. Lett.*, vol. 88, no. 8, 2006, Art. no. 083502.
[10] E. Bosman, G. Van Steenberge, B. Van Hoe, J. Missinne, J. Vanfleteren, and P. Van Daele, "Highly reliable flexible active optical links," *IEEE Photon. Technol. Lett.*, vol. 22, no. 5, pp. 287–289, Mar. 2010.
[11] D. Guidotti, Y. Jianjun, M. Blaser, V. Grundlehner, and G. Chang, "Edge viewing photodetectors for strictly inplane lightwave circuit integration and flexible optical interconnects," in *Proc. 56th Electron. Compon. Technol. Conf.*, 2006, pp. 782–788.
[12] K. Cherenack, K. V. Os, and L. V. Pieterson, "Smart photonic textiles begin to weave their magic," *Laser Focus World*, vol. 48, pp. 63–66, 2012.
[13] Z. Yu, X. Niu, Z. Liu, and Q. Pei, "Intrinsically stretchable polymer light-emitting devices using carbon nanotube-polymer composite electrodes," *Adv. Mater.*, vol. 23, no. 34, pp. 3989–3994, 2011.
[14] J. Yoon *et al.*, "Flexible concentrator photovoltaics based on microscale silicon solar cells embedded in luminescent waveguides," *Nature Commun.*, vol. 2, 2011, Art. no. 343.
[15] J. Yoon *et al.*, "Ultrathin silicon solar microcells for semitransparent, mechanically flexible and microconcentrator module designs," *Nature Mater.*, vol. 7, no. 11, pp. 907–915, 2008.
[16] W. Park and J. Lee, "Mechanically tunable photonic crystal structure," *Appl. Phys. Lett.*, vol. 85, no. 21, pp. 4845–4847, 2004.
[17] Y. Chen, H. Li, and M. Li, "Flexible and tunable silicon photonic circuits on plastic substrates," *Sci. Rep.*, vol. 2, 2012, Art. no. 622.

[18] D. Taillaert, W. Paepegem, J. Vlekken, and R. Baets, "A thin foil optical strain gage based on silicon-oninsulator microresonators," *Proc. SPIE*, vol. 6619, 2007, Art. no. 661914.
[19] L. Fan, L. T. Varghese, Y. Xuan, J. Wang, B. Niu, and M. Qi, "Direct fabrication of silicon photonic devices on a flexible platform and its application for strain sensing," *Opt. Exp.*, vol. 20, no. 18, pp. 20564–20575, 2012.
[20] J. C. Martinez-Anton, H. Canabal, J. A. Quiroga, E. Bernabeu, M. A. Labajo, and V. C. Testillano, "Enhancement of surface inspection by Moiré interferometry using flexible reference gratings," *Opt. Exp.*, vol. 8, no. 12, pp. 649–654, 2001.
[21] L. Ge, X. Wang, H. Chen, K. Qiu, and S. Fu, "Flexible subwavelength gratings fabricated by reversal soft UV nanoimprint," *Chin. Opt. Lett.*, vol. 10, no. 9, pp. 090502–090505, 2012.
[22] D. H. Kim *et al.*, "Epidermal electronics," *Science*, vol. 333, no. 6044, pp. 838–843, 2011.
[23] Z. Ma, "Materials science: An electronic second skin," *Science*, vol. 333, no. 6044, pp. 830–831, 2011.
[24] C. Choi *et al.*, "Flexible optical waveguide film fabrications and optoelectronic devices integration for fully embedded board-level optical interconnects," *J. Lightw. Technol.*, vol. 22, no. 9, pp. 2168–2176, Sept. 2004.
[25] Y. Huang, G. Paloczi, A. Yariv, C. Zhang, and L. Dalton, "Fabrication and replication of polymer integrated optical devices using electron beam lithography and soft lithography," *J. Phys. Chem. B*, vol. 108, no. 25, pp. 8606–8613, 2004.
[26] G. Paloczi, Y. Huang, and A. Yariv, "Free-standing all-polymer microring resonator optical filter," *Electron. Lett.*, vol. 39, no. 23, pp. 1650–1651, 2003.
[27] J. Clark and G. Lanzani, "Organic photonics for communications," *Nature Photon.*, vol. 4, no. 7, pp. 438–446, 2010.
[28] K. J. Kim, J. W. Kim, M. C. Oh, Y. O. Noh, and H. J. Lee, "Flexible polymer waveguide tunable lasers," *Opt. Exp.*, vol. 18, no. 8, pp. 8392–8399, 2010.
[29] H. Song, M. Oh, S. Ahn, W. Steier, H. R. Fetterman, and C. Zhang, "Flexible low voltage electro-optic polymer modulators," *Appl. Phys. Lett.*, vol. 82, no. 25, pp. 4432–4434, 2003.